Topics in Catalysis Vol. 44, No. 3, June 2007 (© 2007)
DOI: 10.1007/s11244-006-0132-4

In situ imaging of electrode processes on solid electrolytes by photoelectron microscopy and microspectroscopy – the role of the three-phase boundary

J. Janek[a,*], B. Luerßen[a], E. Mutoro[a], H. Fischer[a], and Sebastian Günther[b]

[a]*Institute of Physical Chemistry, Justus-Liebig-University, Heinrich-Buff-Ring 58, 35392 Gießen, Germany*
[b]*Department Chemie, Ludwig-Maximilians-Universität München, Butenandtstr. 11, 81377 München, Germany*

The electrochemical polarisation of metal catalyst films on solid electrolyte substrates can basically lead to three different effects: (a) the generation of mobile surface species (spillover) which spread over the catalyst surface and modify the catalytic activity, (b) potential-controlled segregation of impurities in the catalyst and (c) potential-dependent surface energy (electrocapillarity). The generation of spillover species occurs at the three-phase boundary between metal, solid electrolyte and gas phase and is highly localized. The spreading occurs via diffusion and leads to time-dependent and inhomogeneous surface concentrations. The kinetics of the spillover process can only be observed with *in situ* surface-analytical techniques in combination with electrochemical methods which offer sufficient resolution in space and time. Model experiments with UV and X-ray photoelectron emission microscopy (PEEM and SPEM) are summarized and discussed with respect to their relevance for the better understanding of electrochemical promotion in catalysis.

KEY WORDS: spillover; zirconia solid electrolyte; platinum; surface diffusion; electrochemical promotion; NEMCA.

1. Introduction

The electrochemical promotion of catalysis (EPOC) with metal/solid electrolyte systems is experimentally based on the external control of catalytically active surfaces by an applied electrical potential. This phenomenon has been studied extensively over the last 20 years by Vayenas and co-workers [1] and a number of other groups [2–11]. Based on their results, it is generally accepted that EPOC grounds on the electrochemical generation (pumping/spillover) of promoting surface species at electroactive surface sites (three-phase boundary) [12–15]. In the present paper, we will discuss the kinetics of the underlying electrochemical process from a more general point of view, and in particular, consider its investigation by microspectroscopic techniques – aiming for a detailed microscopic picture of the spillover process. We also propose to regard EPOC as one example of a wider approach, i.e. the *electrochemical control of surfaces*, and to consider the electrochemically driven spillover species only as one possible surface effect on polarised electrodes among others.

As shown in figure 1, we can identify at least three basically different physico-chemical effects which may be triggered by the electrical polarisation of a (metal) catalyst surface: (a) spillover ions or atoms may spread over the active surface from the electrochemically active sites of the electrode, (b) the modified chemical potential of the electrochemically pumped component (e.g. oxygen in most cases reported so far) may cause the reversible segregation of impurities in the metal to the catalyst surface and (c) the applied electric potential will change the surface energy of the metal electrode (electrocapillarity) and may cause surface restructuring. Clearly all three phenomena are closely inter-related, and it is virtually impossible to separate them. But all three effects will influence the reactivity of polarised electrodes and have to be taken into account in the study of electrochemically controlled surface reactions. Finally, in the case of an sufficiently high chemical potential (obtained by electrochemical polarisation) the growth of surface and bulk oxides on the electrode can occur, adding further complexity to processes (a), (b) and (c).

Whereas the electrochemical polarisation of conventional immersed electrodes in fluid electrolytes only affects the interface between the electrolyte and electrode material, the polarisation of solid/solid electrodes will always influence both the interface and the free surfaces of electrode and electrolyte. With respect to EPOC the generation of spillover species (see figure 1a) appears to be the dominant factor, at least regarding the extensive work which has been published in the last two decades by a number of research groups. Experimental results on electrochemically controlled segregation (figure 1b) and electrocapillarity effects (figure 1c) of solid electrodes on solid electrolytes have not been reported

* To whom correspondence should be addressed.
E-mail: juergen.janek@phys.chemie.uni-giessen.de

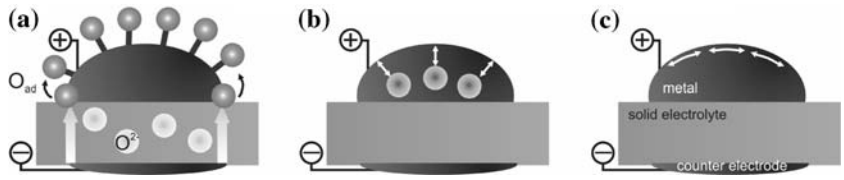

Figure 1. Electrochemical control of metal surfaces by (a) spillover atoms, (b) potential-controlled segregation and (c) electrocapillarity.

yet. The determination of the surface energy and surface tension of solid electrodes in liquid electrolytes, as also the study of the electrocapillary effect, has been critically reviewed by Go and Pyun [16]. First results on the potential-controlled segregation of Si and Fe on Pt/YSZ electrodes were obtained by us recently, but these results require reproduction and will be published elsewhere.

Considering the major experimental techniques which can be applied to the characterisation of electrode processes on solid electrolytes at all, we can group them into the following categories: (a) scanning probe methods (SPM) [17,18] and microelectrodes (μE) [19], (b) photoelectron spectroscopy (PES) [20,21] and emission microscopy (PEEM) [20], (c) IR/Raman microscopy [22,23], (d) X-ray diffraction (XRD) [24], (e) transmission electron microscopy (TEM) [25], environmental scanning electron microscopy (ESEM) [26] and low energy electron diffraction (LEED, no example yet), (f) thermoanalysis (TA) [27] and mass spectrometry (MS) [28], (g) optical methods (ellipsometry, no example yet) and (h) standard electrochemical methods (without SPM and μ-electrodes) [29,30].

Local information – at least on the microscale – is only provided by SPM, μE, PEEM and spatially resolved PES, IR/Raman microscopy, TEM and ESEM – of course with different resolutions. All of them also offer time resolution on different time scales. Studies under atmospheric conditions can yet routinely not be performed with PES/PEEM and TEM, but recent developments aim to overcome this restriction. SPM methods do not require vacuum conditions, but usually vacuum is necessary in order to achieve a sufficient spatial resolution, i.e. imaging quality. Unfortunately just these methods provide the most useful information on the surface chemistry of a given system.

Our experimental approach aims for model-type experiments under *in situ* conditions with microscopic and/or spectroscopic techniques that offer a high resolution in time and space. But as in all catalytic studies, both the material gap and the pressure gap provide serious experimental problems which have to be addressed. The control of atmosphere, temperature and electric potential in a suitable electrochemical cell, in combination with the analytical method, is usually a difficult task, and atmospheric pressure conditions can mostly not be achieved.

Thus, the *in situ* investigation of electrochemical cells and electrodes at intermediate and high temperatures under defined atmospheres with time and spatial resolution is still a developing field, and only a few studies have been reported to date. Among those are reports on FTIR/IRRAS spectroscopy applied to the model system YSZ/Pt(O_2) by Murai *et al.* [31,32], reports by Williams *et al.* on UPS/XPS applied to Cu/Na-β′-alumina electrodes [21] and our own previous studies on Pt/YSZ electrodes [15,20,33,34].

In the present paper we will summarize our own major results on the generation and spreading of spillover oxygen species on platinum electrodes on YSZ solid electrolyte obtained by X-ray and UV photoelectron emission microscopy and microspectroscopy (SPEM and PEEM), emphasizing the influence of the electrode morphology on the spillover processes. Additionally, we will discuss the influence of an electrochemical control of surface segregation – possibly interfering with the spillover process and maybe influencing EPOC. The possible influence of electrocapillarity effects will briefly be discussed at the end of the paper.

2. Evidence for the role of the three-phase boundary

At the three-phase boundary (tpb) the solid electrolyte (SE), the electrode metal and the gas phase meet. It may either be part of a reversible electrode, e.g. in the case of an oxygen-conducting SE in oxygen gas, or of a blocking electrode, e.g. in the case of a porous inert metal electrode on a sodium-conducting SE. The contribution of the tpb to the current across the electrode depends on a number of parameters, including the bulk and surface transport coefficients and the surface reactivities: If the SE itself shows electronic conduction, the reduction or oxidation step can also take place on the SE surface. If the metal is permeable for the reacting gas, the reduction and oxidation step can also take place at the two phase boundary between metal and SE. Thus, the optimization of electrodes requires not only the design of the tpb, but rather of the complete electrode system. Fleig *et al.* analysed this problem for the case of oxide electrodes on solid electrolytes for solid oxide fuel cells by a combined experimental and theoretical study [35,36].

The different points of interest at a solid/solid(gas) electrode and suitable methods for their study are depicted schematically in figure 2. The electrode kinetics is controlled by the tpb and its extension if (i) the electrode material is not permeable for atomic species

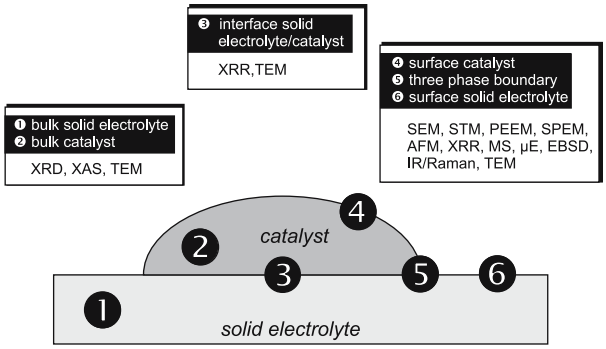

Figure 2. Points of interest around a three-phase boundary in a catalyst/solid electrolyte system and methods for their study. XRR: X-ray reflectometry, XAS: X-ray absorption spectroscopy, STM: scanning tunneling microscopy, EBSD: electron back scatter diffraction.

which participate in the electrode process and/or (ii) if the SE itself provides a sufficiently high electronic conductivity at the surface. Experimental evidence for a significant contribution of the tpb to the kinetics of an electrode can thus be obtained either from systematic phenomenological studies of electrodes with different geometric parameters (variation of electrode area, thickness and tpb length) or by suitable spectroscopic/microscopic studies of the tpb region and the spatio-temporal distribution of the reacting atomic species.

Studies of the influence of the electrode geometry and morphology of metal electrodes on solid electrolytes and the kinetics have mainly been reported by Kenjo *et al.* for Pt/YSZ electrodes [37].

In order to obtain reproducible and quantitative information on the spillover process and its correlation with the tpb by microspectroscopic experiments the following experimental conditions have to be fulfilled:

(a) *Electrode geometry*. The quantitative analysis of the spillover kinetics requires a simple electrode geometry, i.e. the aspect ratio of the electrode should be as small as possible, and the electrode surface should ideally be atomically smooth.

(b) *Electrode microstructure*. As dislocations, grain boundaries and pores are fast diffusion paths for electrochemically pumped species, single crystalline electrodes with a minimum concentration of non-equilibrium defects should be used. Surfaces with high symmetry ((111) or (100)) should be used, in order to allow comparisons with other surface-analytical studies.

(c) *Impurities*. As it is well known that impurities may slowly segregate to the surface during high-temperature experiments, their concentration should be kept as small as possible. In any case, the possible segregation of impurities to the surface or the tpb should be investigated.

(d) *Microspectroscopy*. In order to obtain sufficient experimental data on the spreading of spillover species, the time resolution of the method has to be sufficiently fast, e.g., assuming a surface diffusion coefficient of a spillover species in the order of 10^{-6} cm^2/s, a region within a distance of 100 μm from the tpb is covered with spillover species within a time period in the order of 10^2 s. If a spatial resolution in the order of 100 nm can be obtained, a time resolution in the order 0.1 s is sufficient for the sampling of diffusion profiles.

During the past years we developed a PLD technique for the preparation of thin platinum films on YSZ single crystals which results in well orientated (111), large-grained and dense electrodes (virtually impermeable for oxygen). These electrodes form the materials basis for quantitative study of spillover kinetics. PEEM is the only analytical technique so far which fulfils both the requirements for a sufficient time and spatial resolution. Scanning photoelectron microscopy is still too slow for the sampling of diffusion profiles of spillover species. Only if the spillover spreading can be slowed down by an immobile co-adsorbate, the kinetics can even be studied directly by a method which offers a chemical analysis simultaneously.

3. Experimental techniques

Photoelectron emission microscopy (PEEM) is a mostly non-destructive method for investigations of surfaces in high vacuum ($p < 10^{-6}$ mbar). In PEEM, UV light irradiates the surface and generates photoelectrons from the valence band by the photoelectric effect. The photoelectrons pass an electron optics, the electron optical information is amplified by a channel plate and converted into a two-dimensional visible *in situ* image of the spatial distribution of electron emission on a phosphorous screen. The experimental arrangement is depicted in figure 3.

An important difference to scanning methods is that the whole sample surface is illuminated and an image is recorded directly. The contrast in a PEEM image corresponds to a variation of the electron yield, focusing of electrons into or out of the collection volume of the objective lens-aperture by topographical relief and shading due to the illumination from one side [38]. A variation of electron yield can be caused either by spatial differences in the work function or by electrical or magnetic fields along the sample surface. Reasons for a spatially varying work function can be of chemical origin (different chemical phases or different adsorbates), of crystallographic origin (different crystallographic orientations of the same material possess different work functions) or can be caused by different concentrations of steps and lattice defects.

The depth of the sample region from which the information is acquired, is determined by the free mean path of the electrons and lies in nm range. The lateral spatial resolution of commercial instruments ranges

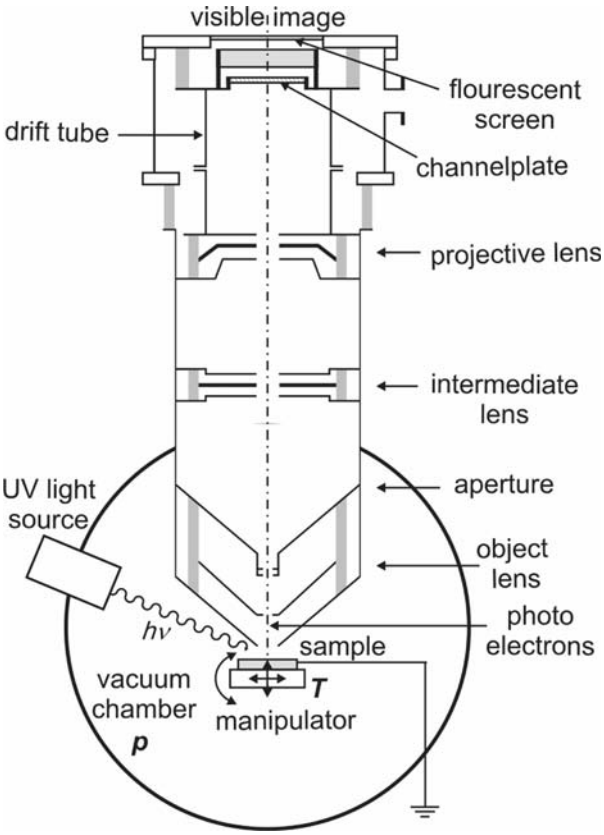

Figure 3. Experimental arrangement of a photoelectron emission microscope for *in situ* studies of electrode systems.

between 10 and 100 nm, the theoretically limited resolution corresponds to approx. 1 nm [39,40].

For a detailed insight into this method we refer to review articles and the references therein [38,40,41]. Typical applications of PEEM in materials and surface science include studies of multi-phase systems in the micrometer and sub-micrometer range and the investigation of the kinetics of surface reactions. Even biological samples have already been studied by PEEM [42].

Scanning photoelectron microscopy (SPEM) usually represents an ESCA experiment with high spatial resolution, which can so far only been used at synchrotron radiation sources (figure 4). For our experiments we use the ESCA Microscopy beamline at ELETTRA/Sincrotrone Trieste, Italy [43,44]. Using a photon energy of approximately 650 eV it allows two modes of operation: first, the spatially resolved XPS spectroscopy from a small spot (diameter ≤ 0.15 μm) and second, imaging the element distribution on the surface by setting the analyser to a kinetic energy specific for a certain element. The spatial resolution of the instrument approximates to 100 nm with a energy resolution of 400 meV. The samples can be heated up to 600 °C under different gas atmospheres, and voltages between −3 V and + 3 V can be applied (using a potentiostat). For a detailed insight into SPEM and to its typical applications we refer to review papers and the references therein [40,45].

Figure 5 shows the three different types of Pt electrodes which we used for our *in situ* measurements: porous electrodes (figure 5a) were prepared by sintering Pt paste at elevated temperatures (750 °C). The high resolution scanning electron microscopy (HRSEM) image shows a microporous structure with particles in the 10 μm range.

Microlithography was used to prepare the microstructured working electrodes. During the process Pt is evaporated and deposited on the solid electrolyte. After a cleaning procedure the electrodes show a nanocrystalline structure as it is visible from the HRSEM picture in figure 5b. Finally, we prepared thin epitaxial Pt films by pulsed laser deposition (PLD) and a subsequent annealing treatment (figure 5c). These electrodes are virtually defect-free over large areas (several micrometers) except for a few droplets unavoidably resulting from the deposition process. Such electrodes allow for the first time the *in situ* study of processes at a defined three-phase boundary.

4. Experimental results

4.1. Anodic polarization – oxygen spillover

For the direct *in situ* observation (imaging) of the oxygen spillover process we used photoelectron emission

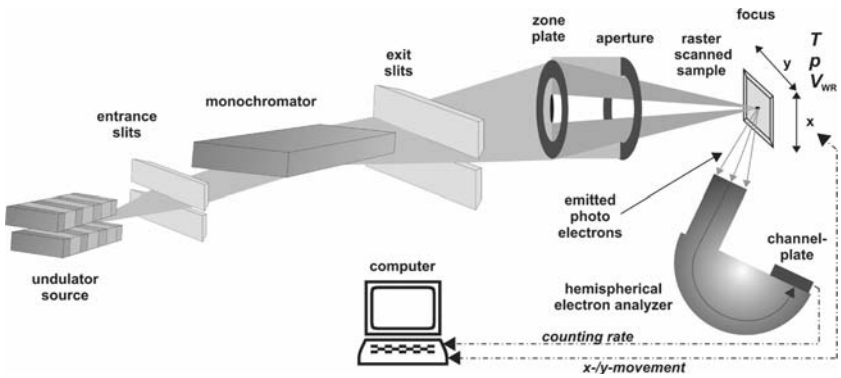

Figure 4. Experimental arrangement of the scanning photoelectron microscope at ELETTRA/Sincrotrone Trieste, Italy, for *in situ* SPEM studies of electrode systems.

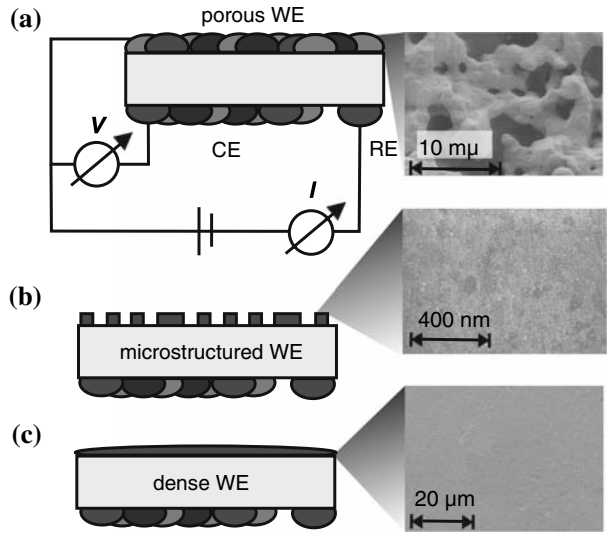

Figure 5. Electrodes model systems and SEM pictures: (a) typical morphology of a sintered Pt paste electrode, (b) sputtered Pt electrode with nanosized grains, (c) thin film Pt electrode prepared by PLD and subsequent thermal ripening. The picture shows an over large areas defect-free electrode.

microscopy (PEEM). Two representative results for different types of electrodes are displayed in figure 6. First, we used two types of polycrystalline platinum electrodes deposited on poly- or single-crystalline YSZ: porous electrodes prepared by using platinum paste and microstructured electrodes prepared by a microlithographic process during which the platinum is vapour-deposited. In both cases the results of the PEEM experiments are the same (as shown in figure 6a): the platinum electrode darkens homogeneously as soon as the anodic voltage ($0\ \mathrm{V} < V_{\mathrm{WR}} \leq +1.5\ \mathrm{V}$) is applied, i.e. the spillover species which increases the work function covers the surface homogeneously within the time resolution of the experiment. The explanation for this behaviour is obviously the microstructure, i.e. the grain size of only a few micrometers. The diffusion lengths are too small for the spatial resolution of the PEEM in the order of 1 μm, and thus, it is not possible to observe the non-stationary surface diffusion profiles of the electrochemically generated oxygen.

A typical result for the third type of platinum electrode we used is shown in figure 6b. As described above, pulsed laser deposition offers the possibility to prepare dense and orientated electrodes (cf. figure 5c) with a well-defined three-phase boundary. The PEEM images in figure 6b show a time series of the same electrode with the platinum electrode on the left side and the YSZ solid electrolyte on the right (dark) side. As soon as the voltage of $V_{\mathrm{WR}} = +0.2\ \mathrm{V}$ is applied oxygen atoms leave the solid electrolyte directly at the tpb between platinum and YSZ and diffuse (''spill'') over the electrode. Since the formation of chemisorbed oxygen on platinum increases the work function of the metal the PEEM image darkens and the diffusional distribution of the oxygen appears as a dark front.

In order to extract the diffusion coefficient of the spillover species, we performed a quantitative analysis of the diffusion profile in figure 6b by relating the local grey values G of the PEEM images to the local spillover concentration. We assumed that $G(x,t)$ is proportional to the photocurrent I, and that the work function ϕ of the Pt electrode scales linearly with the surface coverage $\theta(x,t)$ of oxygen [46]. The relation between I and ϕ is given by the Fowler equation ($I \sim \phi^2$). Additionally we assumed that the maximum coverage of oxygen on Pt(111) corresponds to $\theta = 0.25$ ML [47–49]. The resulting θ–t-curves at a given position were analysed with a solution of Fick's second law of diffusion [50]:

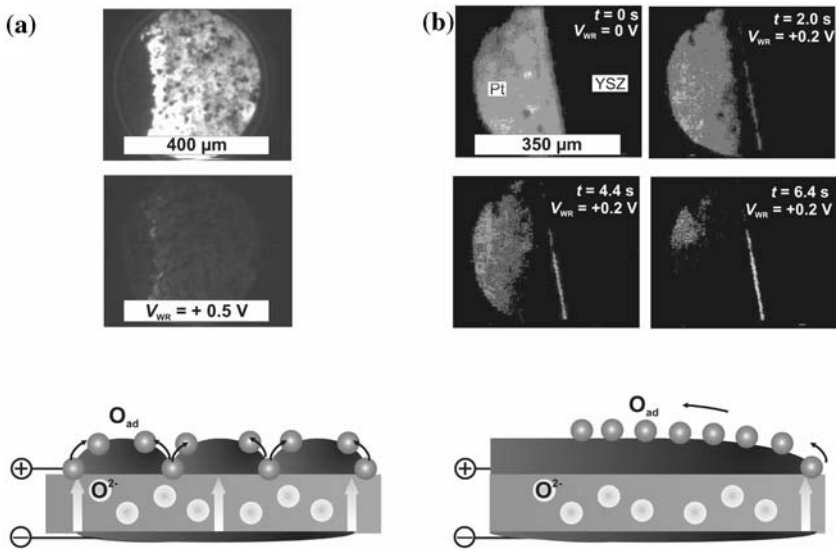

Figure 6. Experimental results for PEEM of Pt electrodes under anodic polarisation and schematic graphs of the spillover process. (a) Polycrystalline ($V_{\mathrm{WR}} = 0.5$ V, $T = 670$ K) and (b) dense electrode ($V_{\mathrm{WR}} = 0.2$ V, $T = 670$ K).

$$N(x,t) = 2q\sqrt{\frac{t}{D}}\left[\frac{1}{\sqrt{\pi}}\exp\left(-\frac{x^2}{4Dt}\right) - \frac{x}{2\sqrt{Dt}}\operatorname{erfc}\frac{x}{2\sqrt{Dt}}\right]$$

Here N denotes the number of oxygen atoms per area (atoms/cm^2), q is the rate of oxygen generation per unit length of the tpb (atoms/cm s) and x is the distance from the tpb (cm). D corresponds to the diffusion coefficient (cm^2/s) and t to the time (s) (figure 7a). The boundary condition is a constant flux of oxygen starting from a linear three-phase boundary. No dependence of the diffusion coefficient on the coverage and no possible desorption of the spillover oxygen are taken into account of the considerations (cf. figure 7a).

For the conversion of N into the coverage θ we made the assumption that 1 ML of adsorbed oxygen on Pt(111) corresponds to 1.5×10^{15} atoms/cm^2 [51]. The experimental data are perfectly described by a fit of the diffusion equation, as shown in figure 7b.

We extracted a diffusion coefficient $D_O = (9.2 \pm 1.8)\times10^{-4}$ cm^2/s at the temperature $T = 670$ K [34]. This value lies between the reported values for oxygen diffusion on single ($D_O = 2\times10^{-9}$ cm^2/s) [51] and polycrystalline ($D_O = 9\times10^{-3}$ cm^2/s) [52] Pt. As the Pt film is not completely free of defects, but rather contains small pores in particular close to the tpb, we expect in fact a larger value of D_O than for a single crystal. At present, orientated and large-grained electrodes with higher quality are investigated systematically. The results will be published elsewhere.

4.2. Cathodic polarization – reduction front

When the working electrode is polarized cathodically the solid electrolyte shows significant changes of its local work function. In figure 8a a sequence of PEEM images of a microstructured platinum electrode is shown during a polarization experiment ($V_{WR} = -0.4$ V). From the second image on the voltage was applied and – starting from the tpb – a bright front propagates and finally covers the whole solid electrolyte. The velocity of the front comes up to a few microns per second.

In the case of a polycrystalline solid electrolyte with platinum paste electrodes a comparable bright front is observed in PEEM. Due to the different transport properties of grain boundaries the front is not as sharp as in the case of single crystalline samples. In any case, these work function fronts are not observed when the polarization experiment is performed in an oxygen atmosphere with $p(O_2) \geq 1\times10^{-7}$ mbar.

The expanding bright region with lower work function represents electrochemically reduced YSZ with Zr-species of lower valence than +4, i.e. with an increased concentration of electrons. The mechanism of this reduction process for bulk material has been discussed earlier [53]. The XPS analysis of the reduced solid electrolyte reveals differences in the behaviour between poly- and single-crystalline YSZ, as discussed in detail in a previous paper [20]. In the case of polycrystalline zirconia two reduced Zr components appear in the Zr 3d spectrum additionally to the Zr^{4+} peak: Zr^0 and – most likely – Zr^{1+}. The Zr^{4+} peak has decreased by a factor of approximately 2. The deconvolution of the Zr 3d peak of the reduced single crystalline YSZ requires also two additional components, namely Zr^{3+} and Zr^{1+}. The complete reduction to Zr^0 species was not observed under our experimental conditions. Thus, the results in [20] clearly show that the single crystalline samples are more resistive to reduction.

4.3. SPEM for the characterisation of spillover species

To date the most of our experimental results suggest that electrochemically generated spillover oxygen is identical to chemisorbed oxygen [15,54], whereas another spectroscopic study by Ladas *et al*. [55] reports an additional oxygen species with a different binding energy. Recent own spectroscopic measurements on thin film platinum electrodes also show additional oxygen signals which cannot be attributed to the normal chemisorbed oxygen with a binding energy of $E_B = 530.4$ eV [56].

We believe that these controversial results are mainly due to severe differences in the chemical composition and microstructure of the platinum electrodes being studied. Despite the fact that the platinum electrode on YSZ plays a major role as an electrochemical model

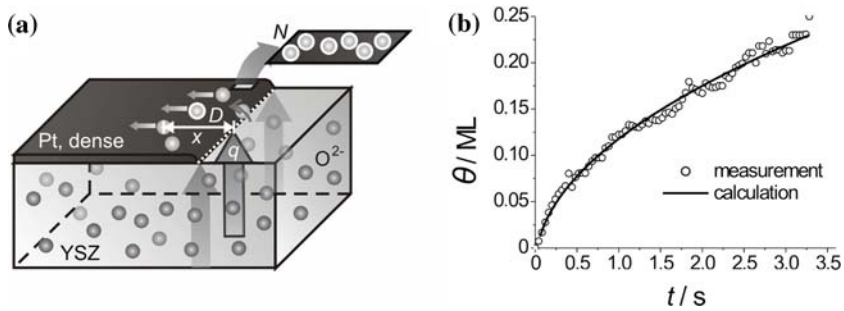

Figure 7. Diffusion analysis of the PEEM result in figure 6b ($V_{WR} = 0.2$ V, $T = 670$ K). (a) Scheme of the diffusion process and (b) θ versus t diagram.

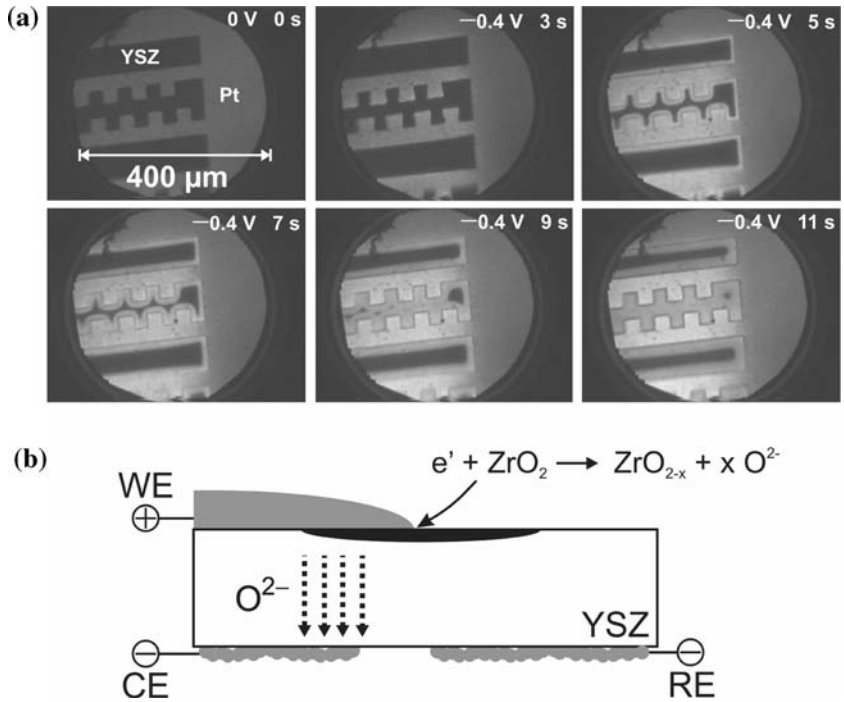

Figure 8. (a) Sequence of PEEM images of a microstructured platinum electrode during cathodic polarization. (b) Schematical graph of the surface reduction of the solid electrolyte.

system, there exists no generally accepted and well reproducible standard preparation for this electrode. The technical standard – sintered Pt electrodes from a metal paste – contains various impurities depending on the supplier. Even worse, despite attempts by Vayenas to document the best sintering route to obtain reasonable porous Pt electrodes, the microstructure of porous Pt electrodes differs significantly from one study to another. Reproducible and unequivocal evidence for the chemical identity of the spillover species will only be obtained if electrodes with a minimum content of impurities and a well-documented microstructure are used for the characterisation with XPS.

We conclude that the current data basis for spillover oxygen is too weak and too controversial for an unequivocal statement on its chemical character. There is evidence that electrochemically generated spillover oxygen on clean platinum surfaces is identical to chemisorbed oxygen. However, we do not exclude the existence of oxygen species with different binding energy and different chemical character – in particular for platinum electrodes with an otherwise unknown impurity content.

In this context it is important to take an electrochemically driven surface segregation of impurities into account. It is well known that the surface segregation of impurities in metals depends on the oxygen activity at the surface [57,58]. Upon electrochemical polarisation the oxygen activity is changed at the tpb and from there it changes along the surface via the mobile spillover species. As a consequence we expect a potential-dependent segregation of impurities, in particular the segregation of less noble metal impurities upon anodic polarisation, and a combination of segregation and spillover effects. We have obtained first experimental evidence on such segregation effects, however, further systematic experiments are required before publication.

4.4. *SPEM for the imaging of spillover diffusion/reaction*

Since the *in situ* observation of the oxygen surface diffusion is only possible using an experimental method like PEEM with a sufficient temporal resolution a direct imaging of the diffusion process with SPEM is not possible (the acquiring of images like the ones shown in figure 9 requires several minutes each). Therefore, a different type of experiment was used to establish an inhomogeneous and quasi-stationary surface distribution of oxygen. By thermal decomposition of ethylene a thin carbon layer was deposited on the platinum electrode. Small holes (diameter in the order of 1 µm) in the platinum electrode formed during the preparation process represent three phase boundaries from where the oxygen can spillover onto Pt sites during electrochemical pumping (cf. figure 9a). Areas with a small number of such holes were chosen for the pumping experiments.

Figure 9b shows three Pt 4f SPEM images (upper row) and the corresponding C 1s images (lower row) at three subsequent times during anodic polarization. Bright areas represent a high concentration of the particular element. As it is clearly visible the carbon is consumed continuously during the experiment, being

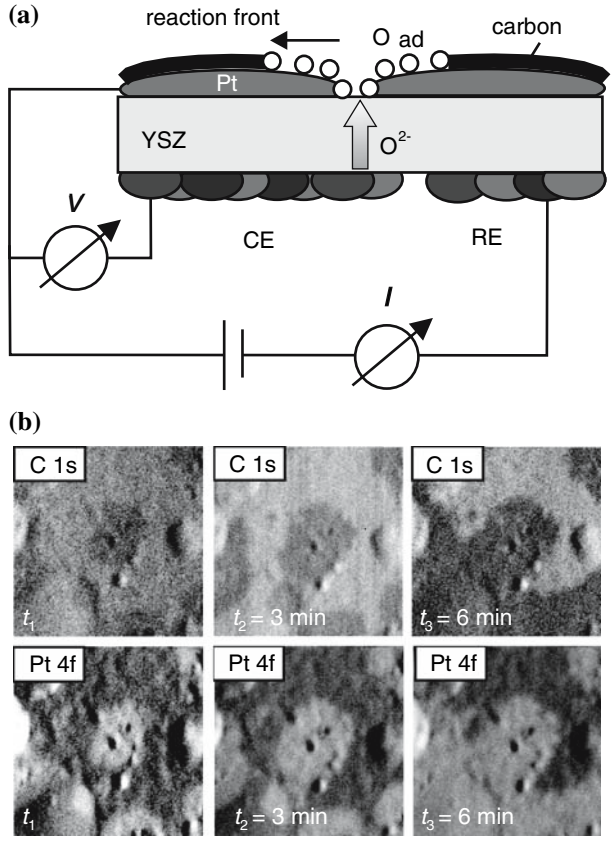

Figure 9. (a) Schematic explanation of an electrochemically controlled surface reaction, (b) Pt 4f (upper row) and C 1s (lower row) SPEM images of a carbon-covered Pt electrode during anodic polarisation (V_{WR} = 0.5 V).

removed by the reaction with the oxygen which is supplied by the holes in the platinum electrode. Thus, the carbon-free areas around the holes grow with time, leading to a clean Pt surface.

When the applied voltage is turned off, the supply of the electrochemically generated oxygen, and thus, the propagation of the reaction front stops immediately. As the reaction of oxygen from the gas phase with the carbon layer is much slower, the carbon remains on the surface until the pumping voltage is turned on again. Thus, it is clearly proven that this experiment is an example of electrochemically triggered surface reaction of spillover oxygen.

5. Discussion

The available experimental data from spectromicroscopic experiments are still scarce but support the general concept of spillover-driven electrochemical promotion – of course without an unequivocal proof for the catalytic effect of the spillover species. For example there is clear and unequivocal evidence that spillover oxygen is generated at the tpb of an electrode. There are also first results on the diffusional spreading of the spillover species. However, systematic results on the dependence of the diffusion coefficient on the experimental conditions and the electrode microstructure are yet not available.

A first example of a chemical reaction between spillover oxygen and a surface layer of carbon has been reported, adding evidence both to the mobility of the species and its reactivity compared to chemisorbed oxygen.

The data on the chemical identity of the oxygen spillover species are still controversial, but this might be caused by differences in the purity and microstructure of the investigated platinum electrodes. An additional complication of electrochemical spillover experiments is probably caused by potential-dependent segregation of impurities. This segregation changes the surface properties during the spillover process and can influence the binding of the spillover species to the surface. Another complication may arise from electrocapillarity effects. However, from our experiments we cannot derive any evidence for an electrocapillarity effect, i.e. for a potential-controlled reversible change of the metal surface. Theoretically, the surface energy of a solid electrode changes upon polarisation. Whether this can lead to microstructural changes of polycrystalline electrodes and to an indirect effect the spillover process has to be answered by future experiments.

6. Outlook

The systematic application of UV–PEEM and SPEM (scanning μ-ESCA) to geometrically and microstructurally well-defined model electrodes will offer a detailed picture of the electrochemically triggered spillover kinetics. The use of electrodes with controlled concentrations of impurities will help to prove and understand the influence of potential-driven surface segregation on the spillover processes. In an additional step these intentionally doped electrodes have to be tested for the electrochemical promotion properties.

If the gas-exposed electrode surfaces represent crystallographic planes with high symmetry, an electrocapillarity effect should not be observed. In contrast, nano- or micro-structured electrodes with a high concentration of different crystallographic surfaces may show morphological changes driven by electrocapillarity. The unequivocal verification of such effect is difficult, as it can a priori not be separated from spillover and segregation effects.

Acknowledgments

Financial support by the DFG (project Ja 648/10-1) is gratefully acknowledged. We thank M. Kiskinova, L. Gregoratti and R. Imbihl for a fruitful cooperation. We thank C.G. Vayenas for continuous and stimulating discussions.

References

[1] C.G. Vayenas, S. Bebelis, C. Pliangos, S. Brosda and D. Tsiplakides, *Electrochemical Activation of Catalysis* (Springer, 2002).
[2] W. Zipprich, H.-D. Wiemhoefer, U. Vohrer and W. Goepel, Ber. Bunsen-Ges. 99(11) (1995) 1406.
[3] J. Nicole and Ch. Comninellis, J. Appl. Electrochem. 28(3) (1998) 223.
[4] S. Völkening, E. Schütz, J. Janek and R. Imbihl, Phys. Chem. Chem. Phys. 1 (1999) 5241.
[5] L. Ploense, M. Salazar, B. Gurau and E.S. Smotkin, Solid State Ionics 136–137 (2000) 713–720.
[6] V.D. Belyaev, T.I Politova and V.A. Sobyanin, Solid State Ionics 136–137 (2000) 721.
[7] M.R. Lambert, A. Palermo, F.J. Williams and M.S. Tikhov, Solid State Ionics 136–137 (2000) 677.
[8] S. Kim and G.L. Haller, Solid State Ionics 136–137 (2000) 693.
[9] D. Poulidi, M.A. Castillo-del-Rio, R. Salar and I.S. Metcalfe, Solid State Ionics 162–163 (2003) 305.
[10] P.M. Leiva and C.G. Sanchez, J. Solid State Electrochem. 7(9) (2003) 588.
[11] J. Fleig and J. Jamnik, Electrochem. Soc. 152(4) (2005) E138.
[12] C.G. Vayenas, S. Bebelis, S. Neophytides, I.V. Yentekakis and Jiang Yi., Stud. Surf. Sci. Catal. 77 (1993) 111.
[13] C.G. Vayenas, R.M. Lambert, S. Ladas, S. Bebelis, S. Neophytides, M.S. Tikov, N.C. Filkin, M. Tsiplakides, D. Cavalc and K. Besocke, Stud. Surf. Sci. Catal. 112 (1997) 39.
[14] G. Foti, I. Bolzonella and Ch. Comninellis, J. Appl. Electrochem. 34 (2004) 9.
[15] B. Luerssen, S. Guenther, S. Marbach, M. Kiskinova, J. Janek and R. Imbihl, Chem. Phys. Lett. 316 (2000) 331.
[16] J.-Y. Go and S.-I. Pyun, J. Korean Electrochem. Soc. 7(4) (2004) 211.
[17] M. Makri, C.G. Vayenas, S. Bebelis, K.H. Besocke and C. Cavalca, Ionics 2(3&4) (1996) 248.
[18] S.P. Jiang and W. Wang, Electrochem. Solid-State Lett. 8(2) (2005) A115.
[19] J. Fleig, Adv. Electrochem. Sci. Eng. 8 (2003) 1.
[20] B. Luerssen, J. Janek, S. Guenther, M. Kiskinova and R. Imbihl, Phys. Chem. Chem. Phys. 4(12) (2002) 2673.
[21] J.F. Williams, A. Palermo, M.S. Tikhov and R.M. Lambert, J. Phys. Chem. B 104(3) (2000) 615.
[22] F. Svegl, B. Orel, V. Kaucic and K. Kalcher, in: *Scientific Papers of the University of Pardubice, Series A: Faculty of Chemical Technology* 3 (1998) 257.
[23] D.I. Kondarides, G.N. Papatheodorou, C.G. Vayenas, X.E. Verykios and X.E. Ber, Buns. Ges. 97(5) (1993) 709.
[24] A.R. Rojas, H.E. Esparza-Ponce, L. Fuentes, A. Lopez-Ortiz, A. Keer and J. Reyes-Gasga, J. Phys. D. Appl. Phys. 38(13) (2005) 2276.
[25] Y.L. Liu and C. Jiao, Solid State Ionics 176(5&6) (2005) 435.
[26] K.-N. Kim, J. Moon, J.-W. Son, J. Kim, H.-W. Lee, J.-H. Lee and B.-K. Kim, J. Korean Ceram. Soc. 42(7) (2005) 509.
[27] S.G. Neophytides, D. Tsiplakides and C.G. Vayenas, J. Catal. 178(2) (1998) 414.
[28] H. Yokokawa, T. Horita, N. Sakai, K. Yamaji, M.E. Brito, Y.-P. Xiong and H. Kishimoto, Solid State Ionics 174(1–4) (2004) 205.
[29] W.-F. Zhang, P. Schmidt-Zhang and U. Guth, Solid State Ionics 169(1–4) (2004) 121.
[30] X.J. Chen, S.H. Chan and K.A. Khor, Solid State Ionics 164(1&2) (2003) 17.
[31] T. Murai, K. Yashiro, A. Kaimai, H. Matsumoto, Y. Nigara, T. Kawada and J. Mizusaki, Trans. Mater. Res. Soc. Jpn. 29(8) (2004) 3439.
[32] T. Murai, K. Yashiro, A. Kaimai, T. Otake, H. Matsumoto, T. Kawada and J. Mizusaki, Solid State Ionics 176(31–34) (2005) 2399.
[33] R. Imbihl and J. Janek, Solid State Ionics 136–137 (2000) 699.
[34] B. Luerssen, E. Mutoro, H. Fischer, S. Günther, R. Imbihl and J. Janek, Angew. Chem. Int. Ed. 45 (2006) 1473.
[35] V. Brichzin and J. Fleig, Solid State Ionics 152–153 (2002) 499.
[36] J. Fleig, J. Power Sources 105(2) (2002) 228.
[37] T. Kenjo, Y. Yamakoshi and K. Wada, J. Electrochem. Soc. 140 (1993) 2151.
[38] M.E. Kordesch, in: *The Handbook of Surface Imaging and Visualization* (ed.) Hubbard A.T. (CRC Press, 1995), Ch. 43.
[39] G.F. Rempfer and O.H. Griffith, Ultramicroscopy 47 (1992) 35.
[40] S. Günther, B. Kaulich, L. Gregoratti and M. Kiskinova, Prog. Surf. Sci. 70 (2002) 187.
[41] M. Mundschau, Ultramicroscopy 36 (1991) 29.
[42] O.H. Griffith, Appl. Surf. Sci. 26(3) (1986) 265.
[43] L. Casalis, W. Jark, M. Kishinova, D. Lonza, P. Melpignano, D. Morris, R. Rosei, A. Savoia, A. Abrami, C. Fava, P. Furlan, R. Pugliese, D. Vivoda, G. Sandrin and F.-Q. Wei, Rev. Sci. Instrum. 66(10) (1995) 4870.
[44] M. Mari, L. Casalis, L. Gregoratti, S. Günther, A. Kolmakov, J. Kovac, D. Lonza and M. Kiskinova, Electron. Spectrosc. Relat. Phenom. 84 (1997) 73.
[45] T. Kinoshita, J. Electron. Spectrosc. Relat. Phenom. 124 (2002) 175.
[46] G.N. Derry and P.N. Ross, J. Chem. Phys. 82 (1985) 2772.
[47] S. Günther, Habilitationsschrift, Universität Hannover (2003).
[48] P.R. Norton, J.A. Davies and T.E. Jackmann, Surf. Sci. 122 (1982) L593.
[49] C. Puglia, A. Nilsson, B. Hernnas, O. Karies, P. Bennich and N. Martensson, Surf. Sci. 342 (1995) 119.
[50] R.B. Banks, in: *Growth and Diffusion Phenomena* (Springer-Verlag, Berlin, Heidelberg, 1994) p. 341.
[51] J.V. Barth, Surf. Sci. Rep. 40 (2000) 75.
[52] M.U. Kislyuk, I.I. Tretykov and R.K. Nartikoev, Kinetika i Kataliz 22 (1981) 1287.
[53] J. Janek and C. Korte, Solid State Ionics 116 (1998) 181.
[54] B. Luerßen, H. Fischer, S. Günther and J. Janek, in: *Proc. of Asian Conf. Solid State Ionics*, Vol. 9, eds. B.V.R. Chowdari, H.-I. Yoo, G.M. Choi and I.-H. Lee (2004) p. 139.
[55] S. Ladas, S. Kennou, S. Bebelis and C.G. Vayenas, J. Phys. Chem. 97 (1993) 8845.
[56] H. Fischer, B. Luerßen, E. Mutoro, S. Guenther and J. Janek, to be published.
[57] R. Danoix-Souchet and A. D'Huysser, Surf. Interf. Anal. 25 (1997) 747.
[58] H.P. Bonzel, A.M. Franken and G. Pirug, Surf. Sci. 104 (1981) 625.